

Parity-odd Neutrino Torque Detection

Hao-Ran Yu,^{1,2,3,*} Ue-Li Pen,^{2,1,4,5,6,†} and Xin Wang^{2,‡}

¹*Tsung-Dao Lee Institute, Shanghai Jiao Tong University, Shanghai, 200240, China*

²*Canadian Institute for Theoretical Astrophysics, University of Toronto, M5S 3H8, ON, Canada*

³*Department of Astronomy, Shanghai Jiao Tong University, Shanghai, 200240, China*

⁴*Dunlap Institute for Astronomy and Astrophysics, University of Toronto, M5S 3H4, ON, Canada*

⁵*Canadian Institute for Advanced Research, CIFAR Program in Gravitation and Cosmology, Toronto, M5G 1Z8, ON, Canada*

⁶*Perimeter Institute for Theoretical Physics, Waterloo, N2L 2Y5, ON, Canada*

(Dated: December 22, 2018)

Cosmological observations are promising ways to improve our understandings of the neutrino mass properties. The upper bound on their sum of mass is given by the cosmic microwave background and large scale structures. These measurements are all parity-even. Here we show that, the presence of neutrino mass provides a unique contribution to the directions of the angular momentum of galaxies, which is the first parity-odd neutrino effect of galaxies or halos. This parity-odd observable is free of the contamination of linear perturbation theory, and can be cleanly separated from other non-gravitational effects. A complete 21-cm survey deep to redshift 1 can give a 5σ confidence level of detecting the neutrino torque effect if the sum of neutrino masses is 0.05 eV.

Introduction.— Neutrino mass is a long-standing physics problem. The flavour oscillation experiments [1] discovered the mass splittings of neutrinos and placed a lower bound of the sum of their mass $M_\nu \equiv \sum_{i=1}^3 m_{\nu_i} \gtrsim 0.05$ eV [2]. The existence of neutrino mass has profound impacts on cosmic evolution, and the current cosmic microwave background observations provide an upper bound of $M_\nu \lesssim 0.12$ eV [3]. At low redshifts, neutrinos become non-relativistic, and contribute to the matter energy density Ω_m in the structure formation. Unlike the majority of matter, the cold dark matter (CDM) and baryons, neutrinos maintain a high velocity dispersion, referred to as “free-streaming”, which reduces their gravitational collapse on small scales. A number of large scale structure (LSS) surveys [4, 5] will improve this upper bound using neutrino effects on LSS, however we usually encounter difficulties in disentangling neutrino effects from other parameters, and in understanding halo bias and cosmic variance. Recently, new nonlinear neutrinos effects on LSS are proposed to give independent measurements on neutrino mass [6–8]. For these effects one needs to carefully separate and exclude the contaminations from non-gravitational contributions. For example, although the neutrino effect on weak lensing power spectrum [4] uses pure gravity, there are a large set of systematics affecting the observations and unclear baryonic effects that can contaminate the neutrino signal. Besides, the amount of information and constraining power of the lensing is limited by the projection onto the 2-dimensional sky. Is there a 3-dimensional measure that is cleanly gravity-driven, to measure the neutrino mass?

The angular momentum direction of galaxies. The *direction* of angular momentum (hereafter *spin*) is readily observable, while the magnitude is not. Majority of

galaxies are disk galaxies, and the rotation axis is perpendicular to the disk [9]. The orientation of the disk is obtained by inclination and parallactic angles (parity-even) and dust absorption, and from the Doppler effect of spectral lines we determine the plus-minus sign of the spin, which is parity-odd. A parity-odd spin measurement cannot be contaminated by the linear perturbation theory. Only gravity affects spin statistics of halos or galaxies at large separations, since baryons do not travel to the distance of the free-streaming of neutrinos.

We present the neutrino torque effect, to modulate the spin of dark matter halos. Here we use halos to represent galaxies. The galaxy spin can be observed to a much larger radii through the radio emission of the gas, and the spin change only very modestly to larger radii [10]. Recent hydrodynamic galaxy formation simulations suggest that, although uncorrelated in amplitude, the spin directions of stellar, cold gas components and CDM halo are strongly correlated (e.g. section 4.2 of [11]). In galaxy clusters, central galaxies and satellites are also found to be aligned with halos [12].

Theory.— In the picture of LSS formation, gravitational instability lets initial density fluctuations form dark matter halos, where galaxies are embedded. In these highly nonlinear structures, uncertainties of halo bias, halo merging history and baryonic mechanisms obstruct us from clearly understanding the statistics like number counts and morphologies. In comparison, the spins of galaxies/halos represent a local probe of gravity, especially contributed from the linear epoch of the structure formation.

The initial halo spin is written in Lagrangian space as $\mathbf{j}_L \propto -\int_{V_L} \mathbf{q} \times \nabla \phi_c d^3\mathbf{q}$, where ϕ_c is the gravitational potential of CDM, \mathbf{q} is the Lagrangian coordinates relative to the center of mass of the protohalo in volume V_L . In the tidal torque theory [13], it can be written as, $\mathbf{j}_T \propto \epsilon \mathbf{I}_q \mathbf{T}_c$, where $\mathbf{I}_q = (I_{ij}) \equiv (\int_{V_L} q_i q_j d^3\mathbf{q})$, $\mathbf{T}_c = (T_{ij}) \equiv (\partial_i \partial_j \phi_c)$ are the protogalactic inertia ten-

* haoran@cita.utoronto.ca

† pen@cita.utoronto.ca

‡ xwang@cita.utoronto.ca

sor and the local tidal shear tensor¹, and $\epsilon = (\epsilon_{ijk})$ is the Levi-Civita symbol to collect the asymmetric components generated by the misalignment between \mathbf{I}_q and \mathbf{T}_c . Here, \mathbf{I}_q and \mathbf{T}_c are parity-even, ϵ is parity-odd, and thus \mathbf{j}_T is parity-odd. In linear perturbation theory, ϕ_c remains constant, so \mathbf{T}_c decays as a^{-2} due to the cosmic expansion, where a is the scale factor. Also, the proto-halo shrinks in size and turns more spherical in shape. A decayed tidal field is hard to torque small and round objects, so the spin are expected to be contributed mostly in the linear regime [14]. If a halo has a merging history, it simply collects disconnected regions in Lagrangian space but conserves their total spin. These concepts can be straightforwardly tested in N -body simulations.

In Lagrangian space, CDM and baryonic matter are torqued by the same gravitational shear, so **their subsequent local evolution should not systematically change their respective spin directions.** For example, baryonic feedback has to conserve angular momentum, unless the baryons are expelled from the galaxy and carry angular momentum away systematically. The dynamical friction between baryons and dark matter can only increase the angular momentum correlation. These all indicate a **high correlation between CDM and baryons (e.g. [11]).**

Massive neutrinos contribute sub-percent fraction of the matter ingredient, and their unique spatial distribution and evolution should contribute a unique torque to **CDM and baryons.** In particular, neutrino density field traces CDM on large scales while their small scale structures are smoothed out by their free-streaming. They contribute a predictable tidal tensor $\mathbf{T}_\nu(m_{\nu_i})$ depending on the their mass [15]. The interplay between \mathbf{I}_q and \mathbf{T}_ν leads to an additional neutrino torque $\mathbf{j}_\nu^T \propto \epsilon \mathbf{I}_q \mathbf{T}_\nu$. Integrated it over the cosmic evolution, we denote the total neutrino modulation of the halo spin as $\mathbf{j}_{\nu 0}^T$ given by the tidal torque theory. **This torque is unique in that, the neutrino free-streaming scale is much larger than the scale to which local nonlinear and baryonic effects can systematically contribute.**

Reconstruction.— The feasibility of predicting neutrino torque relies on the precision reconstruction of \mathbf{I}_q and \mathbf{T}_ν .

Neutrino distribution shares the same Fourier phases of CDM from halo reconstruction [15, 16], but only differs by the ratio of their linear transfer function, depending on the neutrino masses. The reconstruction \mathbf{T}_ν is reliable even if it is applied directly on halos [15], because they are relatively linear even at present epoch.

The reconstruction of \mathbf{I}_q relies on the fact that \mathbf{I}_q and \mathbf{T}_c are highly correlated in Lagrangian space [17, 18], which can be understood that \mathbf{I}_q is a collection of matter to be shell-crossed to form a halo, being parallel with \mathbf{T}_c . The latter depends on a precise reconstruction of

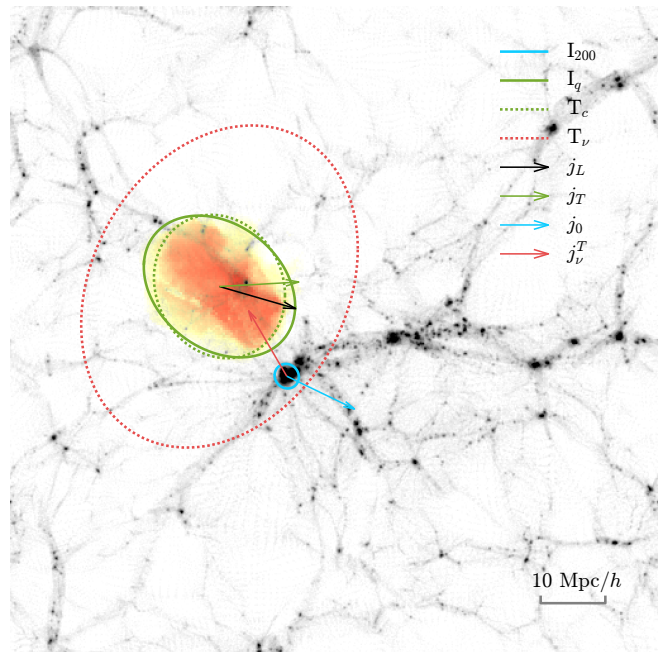


FIG. 1. Visualization of the neutrino torque. We show the LSS slice centered at a selected halo with depth twice the halo radius r_{200} . Equivalent ellipsoids by solid lines show the moment of inertia in Lagrangian and Eulerian space \mathbf{I}_q and \mathbf{I}_{200} , while dotted ellipsoids show the tidal shear from CDM and neutrinos \mathbf{T}_c and \mathbf{T}_ν . \mathbf{j}_L , \mathbf{j}_0 are the Lagrangian and Eulerian halo spins, whereas \mathbf{j}_T is the tidal torque prediction. The initial neutrino torque is shown by \mathbf{j}_ν^T .

CDM initial conditions. Recent years, many emerging reconstruction methods have achieved unprecedented accuracies. For example, the isobaric halo reconstruction [19] can recover the initial conditions of the Universe from spatial distribution of halos. In the case of high halo number densities the reconstructed density field is correlated with the true initial density field on scales $k \lesssim 0.7h/\text{Mpc}$ [16], close to the limit ($k \lesssim 1h/\text{Mpc}$) of isobaric reconstruction from using direct CDM density field [20], or the limit of reconstruction from the true displacement field [21]. ELUCID simulations are able to reconstruct the full evolution history of the real local Universe [22]. These reconstruction techniques enable us to study the tidal field from both CDM and neutrinos in an unprecedented precision, at different epochs of the cosmic evolution. We construct an equivalent inertia \mathbf{I}_R from \mathbf{T}_c , in order to maximize the cross-correlation μ between $\epsilon \mathbf{I}_R \mathbf{T}_\nu$ and $\mathbf{j}_{\nu 0}^T$ (see Appendix A).

The final neutrino torque can be understood as an interaction between two scales – a small collapsing scale \mathbf{T}_c , a large neutrino free-streaming scale \mathbf{T}_ν , and with an antisymmetric (parity-odd) operator ϵ collecting the antisymmetric (parity-odd) contributions from the multiplication of these two symmetric (parity-even) tensors.

Simulation.— These correlations and coefficients are tested across a set of high-resolution N -body simulations

¹ \mathbf{I}_q and \mathbf{T}_c differ from textbook by trace, which does not contribute to \mathbf{j}_T .

[23]. Given any halo formed in the simulation, all the belonging particles are mapped back to Lagrangian space. The status of this definite set of particles can be traced in a resimulation of the exact same initial conditions.

In Fig.1 (all quantities are projected onto the plane of this letter), we select a very massive halo ($7.8 \times 10^{14} M_\odot$) to maximize the clarity of the visualization of the halo properties. We confirm in simulation that these properties (cross-correlations) have only weak dependence on halo mass. The background LSS at redshift $z = 0$ has the thickness $2r_{200}$ with r_{200} being the halo radius within which the mean halo density is 200 times the mean matter density of the Universe. The Lagrangian mapping of this halo is shown by the protohalo's column density with the orange clouds. To visualize the tidal torque theory, we plot equivalent ellipsoids (solid curves) with their moment of inertia equal to \mathbf{I}_q and \mathbf{I}_{200} , where \mathbf{I}_{200} is the moment of inertia within r_{200} . The ellipsoids with dotted lines correspond to \mathbf{T}_c and \mathbf{T}_ν , normalized such that their volumes are V_L and $8V_L$ respectively. As expected, \mathbf{I}_q and \mathbf{T}_c are aligned with their primary axes in parallel with the collapsing direction, perpendicular to the filament containing the halo. Their minor misalignment yields the tidal torque \mathbf{j}_T , which is the first order approximation of the true initial spin \mathbf{j}_L (all the spin arrows are normalized to have 15 Mpc/h). They are, in general, highly correlated with the spin of the final halo \mathbf{j}_0 . In comparison, the neutrino tidal shear \mathbf{T}_ν torques \mathbf{I}_q in an other less correlated direction \mathbf{j}_ν^T .

The validity of the tidal torque formulation is tested by an ensemble average over all halos, across 3 orders of magnitude in mass range ($> 2 \times 10^{12} M_\odot$), and over simulations with different resolutions. As the Universe evolves from the initial condition to $z = 0$, the cross-correlation coefficients $\langle \mathbf{j}(z) \cdot \mathbf{j}_L \rangle$ and $\langle \mathbf{j}(z) \cdot \mathbf{j}_T \rangle$ smoothly decrease from 1 to 0.80, and from 0.75 to 0.69, respectively.

For neutrinos, the first-order tidal torque approximation gives a near perfect (with cross-correlation 0.99) representation of the actual neutrino torque, and it has generally < 0.2 cross-correlates with CDM torques. This is expected in that \mathbf{T}_c dominates locally whereas \mathbf{T}_ν is contributed beyond the neutrino free-streaming scale. These two species, however, have a highly correlated contribution in structure formation. When we consider the gravitational forces that the two species exerted to the protohalo, $\mathbf{F}_{c/\nu} \propto \int_{V_L} \nabla \phi_{c/\nu} d^3q$, the cross-correlation between two species is as high as 0.86.

From simulations, we estimate the magnitude of integrated neutrino torque $\langle |\mathbf{j}_{\nu 0}^T|/|\mathbf{j}_0| \rangle \simeq 3 \times 10^{-4}$. In particular, the effect given by the smoother distribution for neutrinos relative to CDM accounts 0.03, while the neutrino fraction $f_\nu = 3.5 \times 10^{-3}$ (for $M_\nu = 0.05$ eV) and the back-reaction factor from neutrinos to CDM $\sqrt{8}$ [24] contribute the rest.

Measured from simulations, the cross-correlation between $\epsilon \mathbf{I}_R \mathbf{T}_\nu$ and $\mathbf{j}_{\nu 0}^T$ is about $\mu = 0.19$ (see Appendix A). We then need 5×10^9 halos to have a 5σ detection

(see Appendix B). If we improve the reconstruction of \mathbf{I}_R from studying the cosmic evolution history [22], the lower limit of required halos is 2×10^8 .

Discussion.— We proposed a new neutrino observable that has not been considered before. The applicability relies on the new research studies on the angular momentum connection. Galaxy formation simulations like [11, 12] are needed to study the Lagrangian spin correlations for baryons, despite that combining [11] and our result already implies a strong correlation. For galaxy clusters, the correlation between minor axes in [12] also implies the correlation between spins. After all, however, since most galaxies are not in clusters so the contribution of clusters is not a major effect.

We found that the cross-correlation coefficients between \mathbf{j}_0 and initial values \mathbf{j}_L and \mathbf{j}_T are prominently higher than our previous understandings (e.g. [17]). We carefully investigate the numerical errors that may affect the results. P3M (particle-particle particle-mesh) algorithms result in higher cross-correlation between initial and final spins, compared to PM (particle-mesh), where additional tangential forces in PM violate the angular momentum conservation. Higher mass halos in a given simulation generally have slightly higher cross-correlations between initial and final spins, however the correlation is enhanced as we use higher mass resolutions. All other cross-correlation measurements have only weak dependencies on the halo mass, even in a fixed simulation. With different box sizes, mass resolutions, force resolutions, we find that the results are consistent across these simulations. The estimation of number of halo spins needed to detect the neutrino torque depends on $\mu = 0.19$. This has a very weak dependence on halo mass and configuration of the simulation. An accurate study of the neutrino torque requires mass and force resolutions to cover the wide range of halo mass, a large box size (> 600 Mpc/h) to account the neutrino tides at distance, and neutrino particles/fluids, further studies of reconstruction of \mathbf{I}_R (Appendix A) to calculate more precise nonlinear neutrino effects on an evolving halo. These require future simulations with computing power comparable to that of TianNu [25].

Surveys like the Hubble Sphere Hydrogen Survey (HSHS) [26] or a modified 21cm Cosmic Vision [27] are able to observe order of 10^9 HI galaxies ($> 10^{12} M_\odot$), in a cosmic volume $(4\text{Gpc}/h)^3$ below redshift $z \simeq 1$ [28]. Under the standard model of the Universe with $M_\nu = 0.05$ eV, a 5σ detection will be reachable. Beyond standard models, e.g., the neutrino mass could be generated through a neutrino vacuum condensate triggered by a gravitational θ -term [29], the tidal torque history will be different, and we need different numbers of galaxies to differentiate between these models.

Conclusion.— Enormous efforts has been contributed to the neutrino mass properties. Radio astronomic and cosmological surveys are promising low-cost experiments implemented in the Universe to probe basic physics mysteries. The angular momentum is a 3-dimensional,

gravity-driven, parity-odd measure, and is readily observable, well modeled by the tidal torque theory, and well conserved over the cosmic evolution. It contains comparable amount of information as density field but poorly appreciated in application. Recent developed reconstruction techniques enable us to visit an-order-of-magnitude more precise initial conditions of the Universe in Lagrangian space, to accurately reconstruct the neutrino torque effects, and to unveil the neutrino mass properties in upcoming galaxy surveys.

Acknowledgments.— We thank the anonymous referee who gives valuable comments which improved this letter. HRY thanks Derek Inman, Yipeng Jing, Pengjie Zhang and Jiaxin Han for helpful comments and suggestions. We acknowledge funding from NSERC. The simulations were performed on the Sunnyvale cluster at CITA and on the Niagara supercomputer at the SciNet HPC Consortium.

Appendix A: Reconstruction of \mathbf{I}_R

In Lagrangian space, \mathbf{I}_q and \mathbf{T}_c are highly correlated. In linear, intermediate epochs, \mathbf{I}_q is firstly reshaped ac-

cording to the dominating \mathbf{T}_c , thus the linear evolved $\mathbf{T}_\nu(\tau)$ will act on an evolved $\mathbf{I}(\tau)$. Further, $\mathbf{I}(\tau)$ will be affected by nonlinear effects, which are more difficult to predict, however halos are relatively small and their spin directions can hardly be changed dramatically. A deep study of the latter steps above is beyond the scope of this letter. Here we show that, even simplified to the first point above, the total neutrino torque can still be reconstructed.

We construct an equivalent inertia \mathbf{I}_R from \mathbf{T}_c , in order to maximum the cross-correlation coefficient μ between $\epsilon \mathbf{I}_R \mathbf{T}_\nu$ and $\mathbf{j}'_{\nu 0}$. In the primary coordinate of \mathbf{T}_c , \mathbf{T}_c can be eigen-decomposed as $\mathbf{T}_c = \sum_{i=1}^3 \mathbf{T}_c^{\lambda_i}$ and we find $(\alpha_1, \alpha_2, \alpha_3) = (-0.7, 0.7, 0.08)$ (normalized such that $\sum \alpha_i^2 = 1$) and $\mathbf{I}_R \propto \sum_{i=1}^3 \alpha_i \mathbf{T}_c^{\lambda_i}$ optimize μ to be 0.19.

Appendix B: Errors

Consider N halos with their unit spin vector randomly distributed on a 2-dimensional sphere, i.e., $|\mathbf{j}| = 1$ and $\langle \mathbf{j} \rangle = \mathbf{0}$. Adding an additional vector $\epsilon \hat{\mathbf{x}}$ ($\epsilon \ll 1$) to \mathbf{j} and normalize, $\mathbf{j}' = (\mathbf{j} + \epsilon \hat{\mathbf{x}})/|\mathbf{j} + \epsilon \hat{\mathbf{x}}|$, then project \mathbf{j}' onto $\hat{\mathbf{x}}$ and we get $p = \mathbf{j}' \cdot \hat{\mathbf{x}}$. Since $\langle p \rangle = 2\epsilon/3$ and $\sigma(p) = 1/\sqrt{3N}$, an $n\sigma$ detection requires $N = 3n^2/4\epsilon^2$.

-
- [1] Q. R. Ahmad *et al.*, Phys. Rev. Lett. **89**, 011301 (2002).
 - [2] K. A. Olive and Particle Data Group, Chinese Physics C **38**, 090001 (2014).
 - [3] Planck Collaboration *et al.*, arXiv e-prints, arXiv:1807.06209 (2018), 1807.06209.
 - [4] R. Laureijs *et al.*, ArXiv e-prints (2011), 1110.3193.
 - [5] D. Eisenstein and DESI Collaboration, The Dark Energy Spectroscopic Instrument (DESI): Science from the DESI Survey, in *American Astronomical Society Meeting Abstracts*, volume 225 of *American Astronomical Society Meeting Abstracts*, p. 336.05, 2015.
 - [6] H.-M. Zhu, U.-L. Pen, X. Chen, D. Inman, and Y. Yu, Phys. Rev. Lett. **113**, 131301 (2014), 1311.3422.
 - [7] H.-M. Zhu, U.-L. Pen, X. Chen, and D. Inman, Phys. Rev. Lett. **116**, 141301 (2016), 1412.1660.
 - [8] H.-R. Yu *et al.*, Nature Astronomy **1**, 0143 (2017).
 - [9] S. Mao, H. J. Mo, and S. D. M. White, MNRAS **297**, L71 (1998).
 - [10] Wikipedia, Galaxy rotation curve — Wikipedia, the free encyclopedia, 2018.
 - [11] F. Jiang *et al.*, ArXiv e-prints (2018), 1804.07306.
 - [12] S. Shao *et al.*, MNRAS **460**, 3772 (2016), 1605.01728.
 - [13] S. D. M. White, ApJ **286**, 38 (1984).
 - [14] C. Porciani, A. Dekel, and Y. Hoffman, MNRAS **332**, 325 (2002), astro-ph/0105123.
 - [15] D. Inman *et al.*, Phys. Rev. D **92**, 023502 (2015), 1503.07480.
 - [16] Y. Yu, H.-M. Zhu, and U.-L. Pen, ApJ **847**, 110 (2017).
 - [17] J. Lee and U.-L. Pen, ApJ **532**, L5 (2000), astro-ph/9911328.
 - [18] J. Lee and U.-L. Pen, ApJ **555**, 106 (2001), astro-ph/0008135.
 - [19] H.-M. Zhu, Y. Yu, U.-L. Pen, X. Chen, and H.-R. Yu, Phys. Rev. D **96**, 123502 (2017).
 - [20] Q. Pan, U.-L. Pen, D. Inman, and H.-R. Yu, MNRAS **469**, 1968 (2017), 1611.10013.
 - [21] H.-R. Yu, U.-L. Pen, and H.-M. Zhu, Phys. Rev. D **95**, 043501 (2017), 1610.07112.
 - [22] H. Wang, H. J. Mo, X. Yang, Y. P. Jing, and W. P. Lin, ApJ **794**, 94 (2014), 1407.3451.
 - [23] H.-R. Yu, U.-L. Pen, and X. Wang, The Astrophysical Journal Supplement Series **237**, 24 (2018).
 - [24] S. Bird, M. Viel, and M. G. Haehnelt, MNRAS **420**, 2551 (2012), 1109.4416.
 - [25] J. D. Emberson *et al.*, Research in Astronomy and Astrophysics **17**, 085 (2017), 1611.01545.
 - [26] J. B. Peterson, K. Bandura, and U. L. Pen, ArXiv e-prints, astro (2006), astro-ph/0606104.
 - [27] K. Dawson *et al.*, ArXiv e-prints, arXiv:1802.07216 (2018), 1802.07216.
 - [28] M. A. Zwaan *et al.*, MNRAS **350**, 1210 (2004), astro-ph/0406380.
 - [29] G. Dvali and L. Funcke, Phys. Rev. D **93**, 113002 (2016).